© 2019. Published by The Company of Biologists Ltd | Journal of Cell Science (2019) 132, jcs217521. doi:10.1242/jcs.217521

RESEARCH ARTICLE

HsSAS-6-dependent cartwheel assembly ensures stabilization of centriole intermediates

Satoko Yoshiba[1,*], Yuki Tsuchiya[1,2], Midori Ohta[1], Akshari Gupta[1,2], Gen Shiratsuchi[1], Yuka Nozaki[1], Tomoko Ashikawa[1], Takahiro Fujiwara[3], Toyoaki Natsume[4], Masato T. Kanemaki[4] and Daiju Kitagawa[1,2,*,‡]

ABSTRACT

At the onset of procentriole formation, a structure called the cartwheel is formed adjacent to the pre-existing centriole. SAS-6 proteins are thought to constitute the hub of the cartwheel structure. However, the exact function of the cartwheel in the process of centriole formation has not been well characterized. In this study, we focused on the functions of human SAS-6 (HsSAS-6, also known as SASS6). By using an *in vitro* reconstitution system with recombinant HsSAS-6, we first observed its conserved molecular property of forming the central part of the cartwheel structure. Furthermore, we uncovered critical functions of HsSAS-6 by using a combination of an auxin-inducible HsSAS-6-degron (AID) system and super-resolution microscopy in human cells. Our results demonstrate that the HsSAS-6 is required not only for the initiation of centriole formation, but also for the stabilization of centriole intermediates. Moreover, after procentriole formation, HsSAS-6 is necessary for limiting Plk4 accumulation at the centrioles and thereby suppressing the formation of initiation sites that would otherwise promote the development of extra procentrioles. Overall, these findings illustrate the conserved and fundamental functions of the cartwheel in centriole duplication.

KEY WORDS: Centriole, SAS-6, Cartwheel, AID

INTRODUCTION

The centrosome is the main microtubule-organizing center of animal cells. It comprises a pair of centrioles surrounded by pericentriolar material (PCM). Centriole formation is indispensable for centrosome duplication and must be strictly regulated during cell cycle progression to ensure robust formation of bipolar spindles and correct chromosome segregation (Brito et al., 2012; Fu et al., 2015; Godinho and Pellman, 2014; Nigg and Raff, 2009).

Centriole formation starts with the assembly of a cartwheel structure at the proximal wall of the pre-existing centriole, which dictates the 9-fold radial symmetrical arrangement of the centriole (Hilbert et al., 2016; Kilburn et al., 2007; Kitagawa et al., 2011; Nakazawa et al., 2007; van Breugel et al., 2011). Following the initial assembly of cartwheel layers, the peripheral triplet microtubules are attached and distally capped, allowing further centriole elongation and maturation (Gönczy, 2012). In mammalian cells, the cartwheel is detectable throughout procentriole formation, but is absent in the mature mother centrioles in the subsequent G1 phase (Guichard et al., 2010).

Evolutionarily conserved proteins of the SAS-6 family (Dammermann et al., 2004; Leidel et al., 2005) are recognized as a core component of the cartwheel structure (Culver et al., 2009; Guichard et al., 2012; Kitagawa et al., 2011; Nakazawa et al., 2007; Stevens et al., 2010; van Breugel et al., 2011). SAS-6 proteins form rod-shaped homodimers with their coiled-coil domains, and these homodimers are thought to self-assemble with their globular heads oriented towards the central part of the cartwheel (Guichard et al., 2012; Hilbert et al., 2016; Kitagawa et al., 2011; Nakazawa et al., 2007; van Breugel et al., 2011, 2014). In most cells, a lack of SAS-6 proteins results in failure of centriole formation. In *Chlamydomonas* and *Drosophila*, defective centrioles with an aberrant number of triplet microtubules are detectable in the mutants lacking SAS-6 proteins (Nakazawa et al., 2007; Rodrigues-Martins et al., 2007). In fact, 90% of cells mutant for *bld12*, the SAS-6 homolog in *Chlamydomonas*, do not have centrioles, and aberrant centriole symmetries were only seen in a small fraction of the remaining 10% of cells (Nakazawa et al., 2007). Meanwhile, in human cells, a lack of the human SAS-6 (herein denoted HsSAS-6, also known as SASS6) results in the complete failure of centriole duplication (Leidel et al., 2005; Strnad et al., 2007).

Recent reports have further revealed the unique molecular properties of SAS-6 proteins and their essential role in the initiation of centriole duplication (Fong et al., 2014; Keller et al., 2014; Qiao et al., 2012). However, it is still poorly understood whether the self-assembly ability of SAS-6 proteins is conserved in higher eukaryotes, including humans, and how exactly additional factors facilitate their assembly *in vivo*. Furthermore, after the early stages of procentriole assembly, whether the cartwheel is dispensable or otherwise necessary for the maintenance of growing procentrioles remains to be clarified. These questions stem from technical limitations in the use of conventional knockout and RNAi-based knockdown approaches in cultured human cells. Here, we show the exact functions of HsSAS-6 in centriole duplication, via transient removal of endogenous HsSAS-6 in human cells achieved by using the auxin-inducible degron (AID)-based protein degradation system. Although HsSAS-6 was known to be essential for the initiation of cartwheel assembly, we find that it is also required for the maintenance of centriole intermediates. In addition, the presence of HsSAS-6 at procentrioles limits centriolar loading of Plk4 and thus ensures formation of a single procentriole per parental centriole.

RESULTS

HsSAS-6 can self-assemble and form the central part of the cartwheel *in vitro*

Previous studies have demonstrated, through *in vitro* reconstitution, that SAS-6 protein fragments from *Chlamydomonas* and zebrafish

[1]Division of Centrosome Biology, Department of Molecular Genetics, National Institute of Genetics, ROIS, Mishima, Shizuoka 411-8540, Japan. [2]Department of Genetics, School of Life Science, SOKENDAI, Mishima, Shizuoka 411-8540, Japan. [3]Institute for Integrated Cell-Material Sciences (WPI-iCeMS), Kyoto University, Kyoto 606-8501, Japan. [4]Molecular Cell Engineering Laboratory, Department of Chromosome Science, National Institute of Genetics, ROIS, Mishima, Shizuoka 411-8540, Japan.
*Present address: Laboratory of Physiological Chemistry, Graduate School of Pharmaceutical Sciences, The University of Tokyo, Hongo, Tokyo 113-0033, Japan.

‡Author for correspondence (dkitagawa@mol.f.u-tokyo.ac.jp)

M.T.K., 0000-0002-7657-1649; D.K., 0000-0003-2509-5977

Received 6 March 2018; Accepted 28 May 2019

Journal of Cell Science (2019) 132, jcs217521. doi:10.1242/jcs.217521

form the central hub of the cartwheel structure (Kitagawa et al., 2011; van Breugel et al., 2011). However, we found that HsSAS-6 failed to self-assemble to form the central part of the cartwheel structure under the same conditions (data not shown). Therefore, we next attempted to examine whether HsSAS-6 is also the core component of the cartwheel structure in humans. Considering that the N-terminal globular domain of SAS-6 family proteins, which is required for self-oligomerization, is highly conserved among species (the K_d values of N–N self-interaction of SAS-6 family proteins are 50, 90, 60 and 110 µM for human, zebrafish, *Chlamydomonas* and *C. elegans*, respectively) (Kitagawa et al., 2011; van Breugel et al., 2011), we speculated that HsSAS-6 self-assembly could be induced by promoting protein–protein interactions under concentrated conditions. Lipid monolayers have been used not only for the formation of two-dimensional crystals of soluble proteins, but also for reconstitution of the early stages of endocytosis (Chiu, 1997; Ford et al., 2001, 2002; Lévy et al., 1999). We therefore employed the lipid monolayer system to test whether we could promote HsSAS-6 self-assembly *in vitro* (Fig. S1). Purified HsSAS-6 NL fragments [amino acids (aa) 1–487], which contain the N-terminal globular head and long coiled-coil domain were observed after performing the lipid monolayer assay and negative staining electron microscopy (Fig. 1A–F; Fig. S1). Intriguingly, we found that a ring-like structure had locally assembled from the HsSAS-6 NL fragments on the layer (Fig. 1C). In contrast, we could not find any such structures with the HsSAS-6 F131E mutant proteins, which are defective in the self-assembly through their N-terminal heads (data not shown) (Keller et al., 2014; Kitagawa et al., 2011). Furthermore, the mean diameter of the rings (21.7±1.8 nm) and the mean angle between the spokes (41.9±9.6°) were in good agreement with those previously reported for 9-fold symmetric cartwheel structures *in vitro* (Fig. 1D–F) (Kitagawa et al., 2011; van Breugel et al., 2011). Notably, this is the first evidence that HsSAS-6 proteins can also self-assemble to form the hub of the cartwheel structure *in vitro*. Thus, our data strongly support previous studies indicating that self-oligomerization of SAS-6 is a conserved molecular property that is necessary for cartwheel assembly.

Super-resolution mapping of Plk4, STIL and HsSAS-6 in the process of centriole formation

The oligomerization ability of HsSAS-6 is essential for centriole formation (Kitagawa et al., 2011), but additional factors are thought to be required to facilitate cartwheel assembly *in vivo*. It has previously been suggested that procentriole formation starts with the interaction between Plk4 and STIL and the associated phosphorylation of STIL by Plk4, which is followed by HsSAS-6 loading to the assembly site of procentrioles (Arquint et al., 2015; Dzhindzhev et al., 2014; Kratz et al., 2015; Moyer et al., 2015; Ohta et al., 2014). These proteins are present at the proximal end of procentrioles throughout the growth of the centrioles, until they are removed during mitosis (Arquint and Nigg, 2014; Strnad et al., 2007). To understand the detailed process of the cartwheel assembly in cells, with a focus on centriolar HsSAS-6, we mapped the precise localization of Plk4, STIL and HsSAS-6 at the super-resolution level by using gated stimulated emission depletion (STED) microscopy. As expected, we observed similar localization patterns for these three proteins at the centrioles, relative to the reference markers Cep192 and polyglutamylated tubulin (Fig. 2A). Notably, we also found that Plk4, STIL and HsSAS-6 exhibited unique behavior during procentriole formation: the three proteins started to localize at the procentriole assembly site on the mother centriole wall (denoted stage II in Fig. 2), elongated (stage III) and then finally separated into two parts (stage IV) (Fig. 2A,B). This observation raises the possibility that these proteins exist in two different states, one between mother and procentrioles as a part of 'connecting stalk' (Guichard et al.,

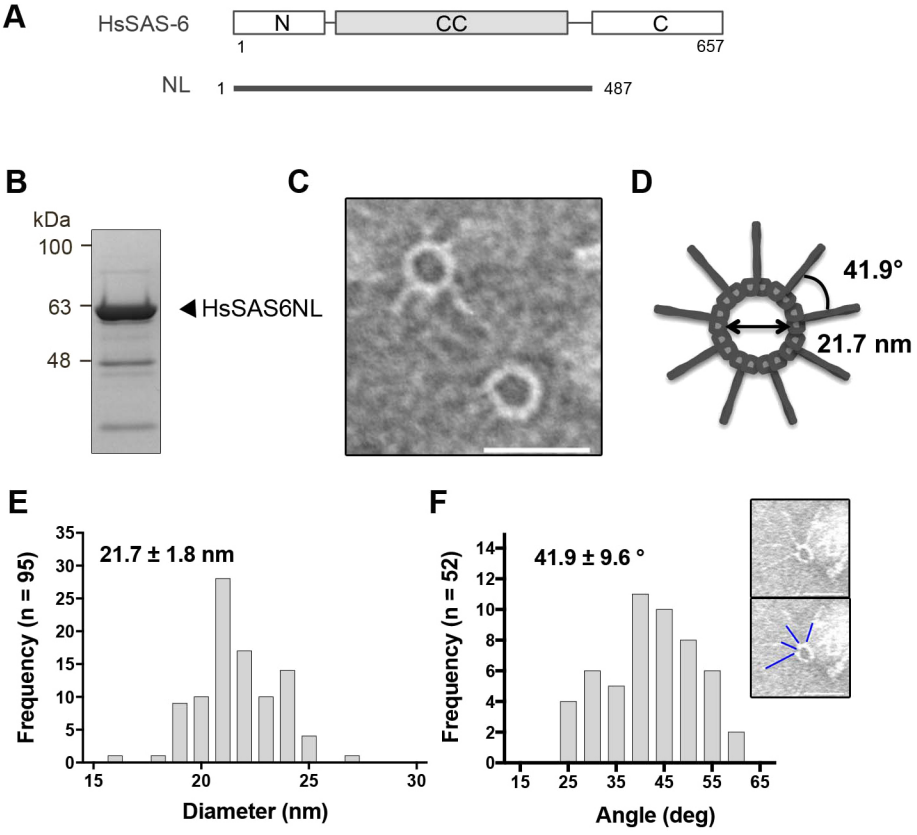

Fig. 1. *In vitro* reconstitution of a central part of the cartwheel structure with HsSAS-6 recombinant proteins. (A) Schematic representation of the HsSAS-6 fragment NL (N-long; aa 1–487) used for *in vitro* reconstitution. (B) The purification of the HsSAS-6 NL fragment was tested by SimplyBlue Safe staining. (C) Representative negative stain electron micrograph of HsSAS-6 NL. The assembly of protein complexes was promoted on a lipid monolayer and mounted onto an EM grid. See detailed method in Materials and Methods and Fig. S1. Scale bar: 50 nm. (D) Schematic interpretation of *in vitro* reconstitution of HsSAS-6 NL. The mean diameter of the rings (21.7 nm) and the mean angle between two spokes (41.9°) are shown. (E) Histogram representation of diameters measured from HsSAS-6 NL rings as shown in C (n=95). (F) Histogram representation of angles measured between two spokes, as indicated with blue lines in the inset, law data above and lined below (n=52). Adjacent spokes that can be distinguished were selected for the measurement because some spokes were too distorted to measure the angle. The values shown in E and F are the mean±s.d.

Journal of Cell Science (2019) 132, jcs217521. doi:10.1242/jcs.217521

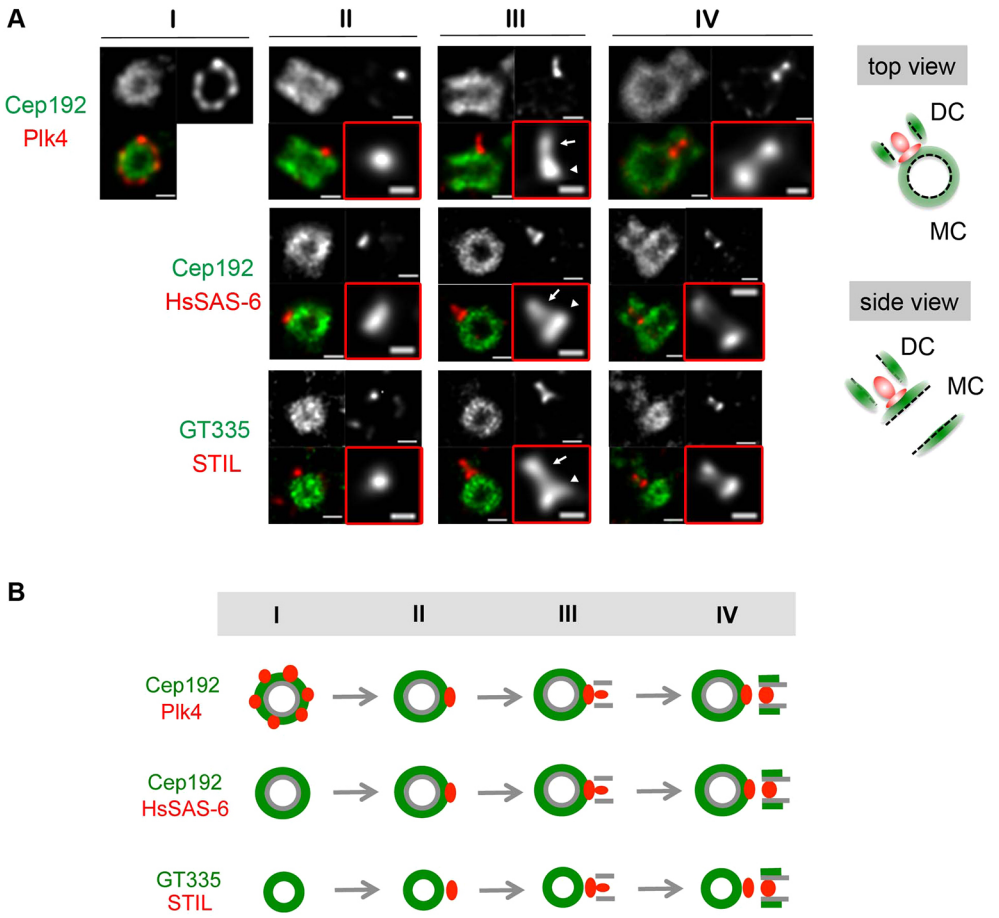

Fig. 2. Super-resolution mapping of Plk4, STIL and HsSAS-6 during the process of procentriole formation. (A) STED images showing the patterns of Plk4, STIL and HsSAS-6 (red) in cycling U2OS cells. Cep192 or polyglutamylated tubulin (GT335) was used for visualizing the centriole walls (green). Note that Cep192 and GT335 appear at daughter centrioles only in the late phase of centriole formation. These pictures were obtained from asynchronous cells and hypothetically rearranged as a sequence of events. Insets outlined in red show enlarged images of the Plk4, STIL and HsSAS-6 pattern. The patterns are classified into 4 types (I–IV) as shown in B. White arrowheads indicate signals located in between mother and daughter centrioles and white arrows indicate signals at the cartwheel structure in daughter centrioles. Normal interphase HCT116 cells were also confirmed to show similar patterns of HsSAS-6 and Cep192. Scale bars: 200 nm (main images); 50 nm (insets). Schematic illustrations of top and side views from mother centrioles are shown on the right. MC, mother centriole; DC, daughter centriole. (B) Schematic representation of pattern classification; I, before STIL/HsSAS-6 loading; II, cartwheel structure formation; III, cartwheel/centriole elongation; and (IV) centriole maturation and separation. Note that Plk4, STIL and HsSAS-6 behave similarly after daughter centriole formation starts (II–IV).

2010), and the other at the base of the procentriole as a part of the 'cartwheel' (Guichard et al., 2010). Interestingly, we also found, under super-resolution, that before STIL and HsSAS-6 loading, Plk4 was distributed as discrete dots, as opposed to a continuous ring, around the mother centriole (Fig. 2A,B). Overall, our data suggest that Plk4, STIL and HsSAS-6 assemble and continue to associate with each other closely throughout centriole duplication.

Establishment of the HsSAS-6-AID human cell line

Although the cartwheel structure is known to be essential for the initiation of procentriole formation, whether it has an additional role in the subsequent processes of procentriole formation remained to be elucidated, presumably because of technical limitations. Therefore, to investigate the possible functions of the cartwheel structure in each step of procentriole formation, we generated an HsSAS-6-AID human cell line, which enabled swifter removal of endogenous HsSAS-6 proteins than the conventional reverse-genetic approach of RNAi. We applied a combination of genome editing by CRISPR/Cas9 and the AID-based protein degradation systems to human HCT116 cells (Natsume et al., 2016; Nishimura et al., 2009; Ran et al., 2013). In an HCT116 cell line constitutively expressing *Oryza sativa* (os)TIR1 (Natsume et al., 2016), which is an essential component of the SCF/E3 ligase required for AID-based degradation, both endogenous HsSAS-6 alleles were AID-tagged at their C-terminal ends (Fig. S2A,B). We note that even in the HsSAS-6-AID cell line even without auxin treatment, there are lower protein expression levels of HsSAS-6-AID compared to the endogenous HsSAS-6 expression levels in the unmodified HCT116 cell line (Fig. 3D; Fig. S2E). This may be because constitutively expressed TIR induces a leaky degradation of HsSAS-6-AID, and/or because the AID tag itself affects the stability of the protein. Nevertheless, the expression levels of *HsSAS-6* mRNA and centrosome duplication in the HsSAS-6-AID cells were not significantly affected, although the cell cycle profile of the HsSAS-6-AID cells shows a slight accumulation in G1 compared to WT cells (Fig. S2C,F–H). We cannot rule out the possibility that the slight cell cycle delay might stem from the reduced amount of total HsSAS-6, or a compromised function for HsSAS-6 resulting from the AID tag. We next confirmed that HsSAS-6-AID protein localized at centrioles, and that the intensity of centriolar HsSAS-6 significantly decreased after 6 h of treatment with indole-3-acetic acid (IAA; natural auxin) (89% decreased) (Fig. 3A,B; Fig. S2D).

We further tested the degradation properties of HsSAS-6-AID proteins in these cells. We found that after addition of IAA, the level of cytoplasmic HsSAS-6-AID proteins was quickly reduced (within 1 h), whereas it took 6 h to completely remove HsSAS-6-AID proteins from the centrioles (Fig. 3C,D). This observation implies that HsSAS-6 proteins that are incorporated into the centriole structure might be more difficult to access and target for protein degradation. Next, we examined whether centriole duplication occurs when HsSAS-6-AID is degraded before centriole formation starts in the late G1 phase. HsSAS-6-AID cells were synchronized in the G2/M phase by treatment with nocodazole, released and then simultaneously treated with IAA until the S phase or the next G1 phase (Fig. 3E–I). The recruitment of HsSAS-6-AID to the centriole was inhibited as a result of the addition of IAA (−IAA 80%, +IAA 0%; Fig. 3F,G), and centriole duplication was effectively blocked when assessed by monitoring recruitment of centriole markers,

Journal of Cell Science (2019) 132, jcs217521. doi:10.1242/jcs.217521

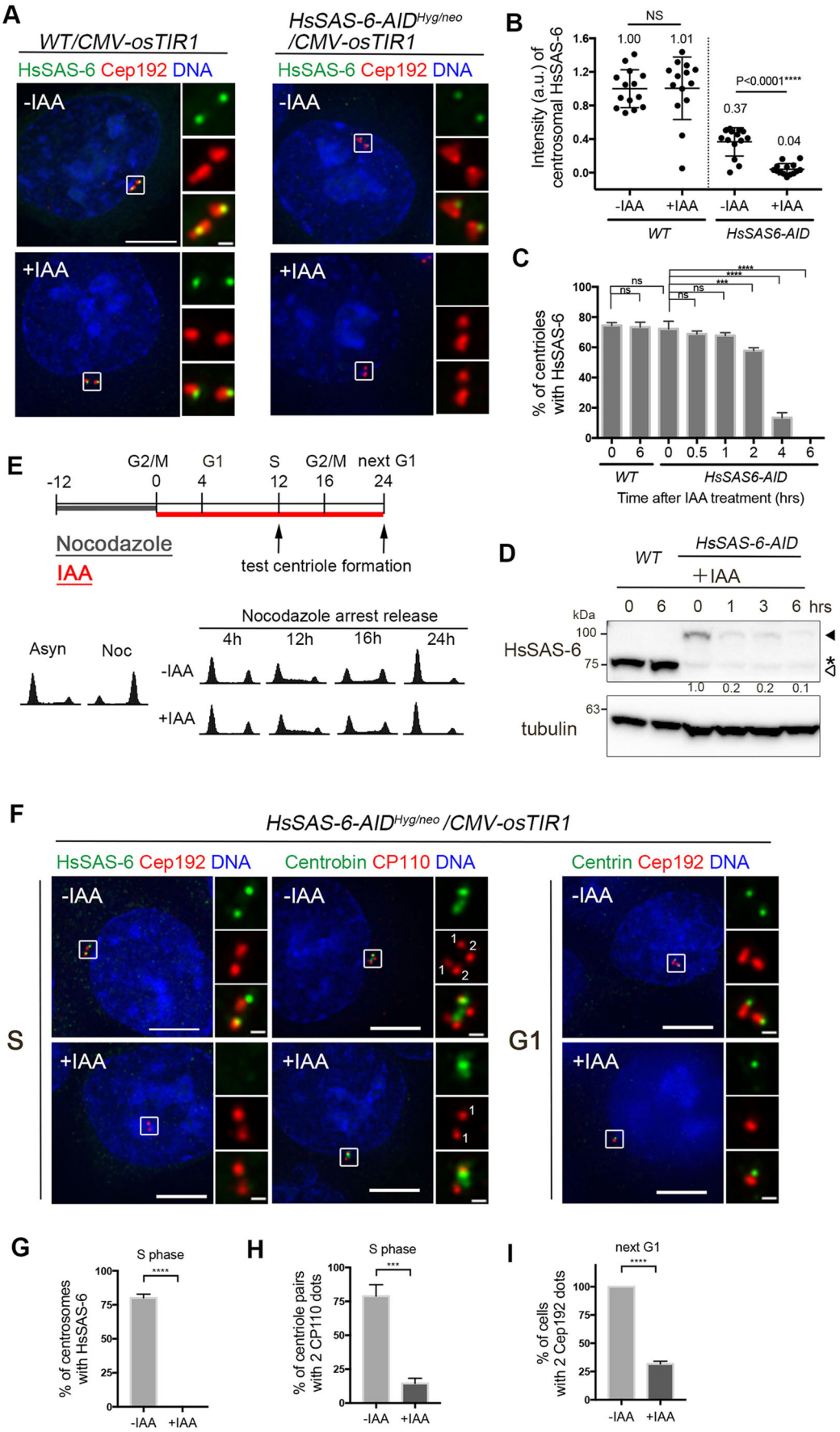

Fig. 3. See next page for legend.

Journal of Cell Science

Journal of Cell Science (2019) 132, jcs217521. doi:10.1242/jcs.217521

Fig. 3. Establishment of the HsSAS-6-AID cell line. (A) Localization of HsSAS-6 (green) and response to IAA (0.5 mM) treatment for 6 h in wild-type (WT) HCT116 cells (left) and HsSAS-6-AID cells (right) are shown. Enlarged views of the boxed region are shown on the right. Scale bars: 10 µm (main images); 0.5 µm (magnifications). (B) The signal intensities (a.u., arbitrary units) of centriolar HsSAS-6 were quantified in of WT and HsSAS-6-AID interphase cells, with and without IAA treatment for 6 h. The values of cytoplasmic signals were subtracted from those of centriole signals, and the subtracted values were analyzed. Each number above the plot indicates the mean intensity of 14 samples from two independent experiments. Error bars indicate the s.d. ****P<0.0001; NS, not significantly different (P>0.05) (two-tailed unpaired t-test). (C) WT and HsSAS-6-AID cells were treated with 0.5 mM IAA, and the number of centrioles with HsSAS-6 at the indicated time points was counted. Values are mean±s.d. percentages from three independent experiments (n≥50 for each condition). ***P<0.001; ****P<0.0001; ns, not significantly different (P>0.05) (one-way ANOVA). (D) The amount of cytoplasmic HsSAS-6 protein was tested in WT and HsSAS-6-AID cells at the indicated time points after IAA treatment. Total lysates were analyzed by western blotting using the indicated antibodies. White and black arrowheads point to endogenous HsSAS-6 and HsSAS-6-AID bands, respectively. The asterisk indicates a non-specific band. Numbers under HsSAS-6 blot indicate the intensities of HsSAS-6-AID bands. Note that the expression level of HsSAS-6-AID was less than that of endogenous HsSAS-6 even before IAA treatment (0 h). (E) Experimental scheme for cell synchronization of HsSAS-6-AID cell line. Cells were arrested in the G2/M phase through treatment of 100 nM nocodazole for 12 h, and were then released and treated with 0.5 mM IAA simultaneously, and collected at the indicated time points to test centriole formation. Cell cycle progression at each time point was monitored by flow cytometry (below). (F) Centriole formation was tested by immunofluorescence using the indicated antibodies. Enlarged images of boxed regions are shown on the right. The numbers in the insets show the number of CP110 spots in one centriole. Scale bars: 10 µm (main images); 0.5 µm (magnifications). (G–I) The numbers of cells with centrosomal HsSAS-6 (G) and centriole pairs with two CP110 dots at S phase (H), and two Cep192 dots in the next G1 phase (I) with and without IAA addition were quantified, respectively. Some cells appear to generate centrioles (CP110, 14%; Cep192, 32%) without HsSAS-6-AID, but this might happen because the cell cycle synchronization by nocodazole arrest-release was not complete, and some cells were arrested at G1 phase right after release, or arrested in S or G2 phase, due to the damage from long-time nocodazole treatment. Values are mean±s.e.m. percentages from three independent experiments (n≥50 for each condition). ***P<0.001; ****P<0.0001 (two-tailed unpaired t-test).

specifically CP110 (also known as CCP110) in S phase (−IAA 79%, +IAA 14%; Fig. 3F,H), and centrin (centrin 1) and Cep192 in the next G1 phase (−IAA 100%, +IAA 32%; Fig. 3F,I), respectively. These results indicate that HsSAS-6-AID degradation induced by IAA before the initiation of centriole formation causes centriole duplication failure, as is the case with HsSAS-6 depletion in RNAi experiments (Leidel et al., 2005; Strnad et al., 2007). Overall, our results confirm that HsSAS-6 is required for the initiation of centriole formation. Additionally, we established the HsSAS-6-AID cell line, in which endogenous HsSAS-6-AID can be rapidly knocked down at the protein level.

HsSAS-6-AID removal from the centriole in the process of procentriole formation

Next, we sought to analyze whether HsSAS-6 is dispensable after the early stages of procentriole assembly, or alternatively whether it is essential for further elongation (Fig. 4B). To examine procentrioles, which are partially formed as intermediate structures, we synchronized cells in the early S phase by using a double thymidine block (DTB) (Fig. S3A). We first confirmed that HsSAS-6 was recruited to most of the centrioles, and that the capping protein CP110 was largely incorporated into the procentrioles (HsSAS-6, 97%; CP110, 79%; Fig. S3B). The lengths of the procentrioles in the early S phase were significantly shorter than those of the fully elongated procentrioles in the G2/M phase, when tested by measuring the distance between CP110 in the mother and procentrioles (0.52 µm at early S, and 0.75 µm at G2/M; Fig. 4A). On the other hand, human (h)Poc5, which only appears in fully elongated, mature procentrioles (Azimzadeh et al., 2009), had not yet been recruited to the procentrioles in the early S phase (0%, Fig. S3B).

Given that it normally takes 6 h to remove HsSAS-6-AID proteins from the centrioles in asynchronous cells (Fig. 3C), we arrested cells in the early S phase, and then treated them with 0.5 mM IAA to remove HsSAS-6-AID from centrioles for the next 6 h prior to analysis (Fig. S3A). Contrary to our expectation, we found that the centrioles remained very weakly stained with HsSAS-6 in 65% of the cells, even in the S-phase arrested cells after 6 h of IAA treatment (Fig. S3C–E). This is presumably because of continuous loading of HsSAS-6 at centrioles during the extended S phase. Hence, HsSAS-6 that is stably incorporated in the centriole structure may be difficult to efficiently target for protein degradation. Centriolar loading of HsSAS-6 is known to be dependent on Plk4 kinase activity (Dzhindzhev et al., 2014; Ohta et al., 2014). Therefore, to completely remove HsSAS-6 from the centrioles, we combined IAA treatment with simultaneous transient Plk4 inactivation via the addition of centrinone (Wong et al., 2015), a Plk4-specific inhibitor (Fig. 4C; Fig. S3F). We found that the addition of 0.5 mM IAA and 100 nM centrinone for 3 h in the early S phase or for 4 h in mid-S phase, was sufficient to remove HsSAS-6 from the centrioles (Fig. 4D–F; Fig. S3G).

After release from DTB in the early S phase, centriole duplication was complete in control cells as shown by the number of Cep192, γ-tubulin and NEDD-1 foci in the next G1 phase (94% duplicated; Fig. 4G; Fig. S3H). We found that in the cells treated with IAA and transiently with centrinone, the number of cells with duplicated centrioles was dramatically decreased in the next G1 phase (24% duplicated; Fig. 4G; Fig. S3H). By contrast, in the cells only treated transiently with centrinone, 81% of the procentrioles became mature centrioles in the next G1 phase, indicating that transient Plk4 inactivation itself affected procentriole formation less (Fig. 4G).

We then sought to investigate the effect of HsSAS-6 removal in the mid S phase, by releasing cells from DTB for 3 h and arresting them again through the addition of thymidine, IAA and centrinone for 4 h to remove HsSAS-6 (Fig. 4C; Fig. S3F). In this experiment, we found that the number of duplicated centrioles in the next G1 phase was dramatically increased compared with what was seen in the case of HsSAS-6 removal in early S phase (83% duplicated; Fig. 4H; Fig. S3H). Taken together, these data suggest that HsSAS-6, and probably the cartwheel structure, are necessary for the integrity of procentriole intermediates at least up to the early S phase, but are thereafter dispensable for subsequent centriole elongation and maturation (Fig. 4I,J).

The intermediate structures harboring cartwheel structures that were observed in DTB-arrested cells were reminiscent of the proximal half of procentrioles formed in Cep295-depleted cells (Chang et al., 2016; Tsuchiya et al., 2016). Cep295 is a conserved protein that is not required for the initiation of cartwheel assembly, but is necessary for the proper elongation and maturation of centrioles through recruitment of Cep135, Cep192, Cep152 and other PCM proteins (Chang et al., 2016; Fu et al., 2016; Saurya et al., 2016; Tsuchiya et al., 2016). Among these proteins, Cep135, also known as Bld10 in *Chlamydomonas* (Matsuura et al., 2004), binds to the C-terminus of HsSAS-6, presumably to promote procentriole formation in human cells (Lin et al., 2013). However, the precise time of the centriolar loading of Cep135 and its functions are still controversial.

Considering the above, we examined the localization patterns of these proteins using super-resolution microscopy (Fig. S4A–D,F,G).

Journal of Cell Science (2019) 132, jcs217521. doi:10.1242/jcs.217521

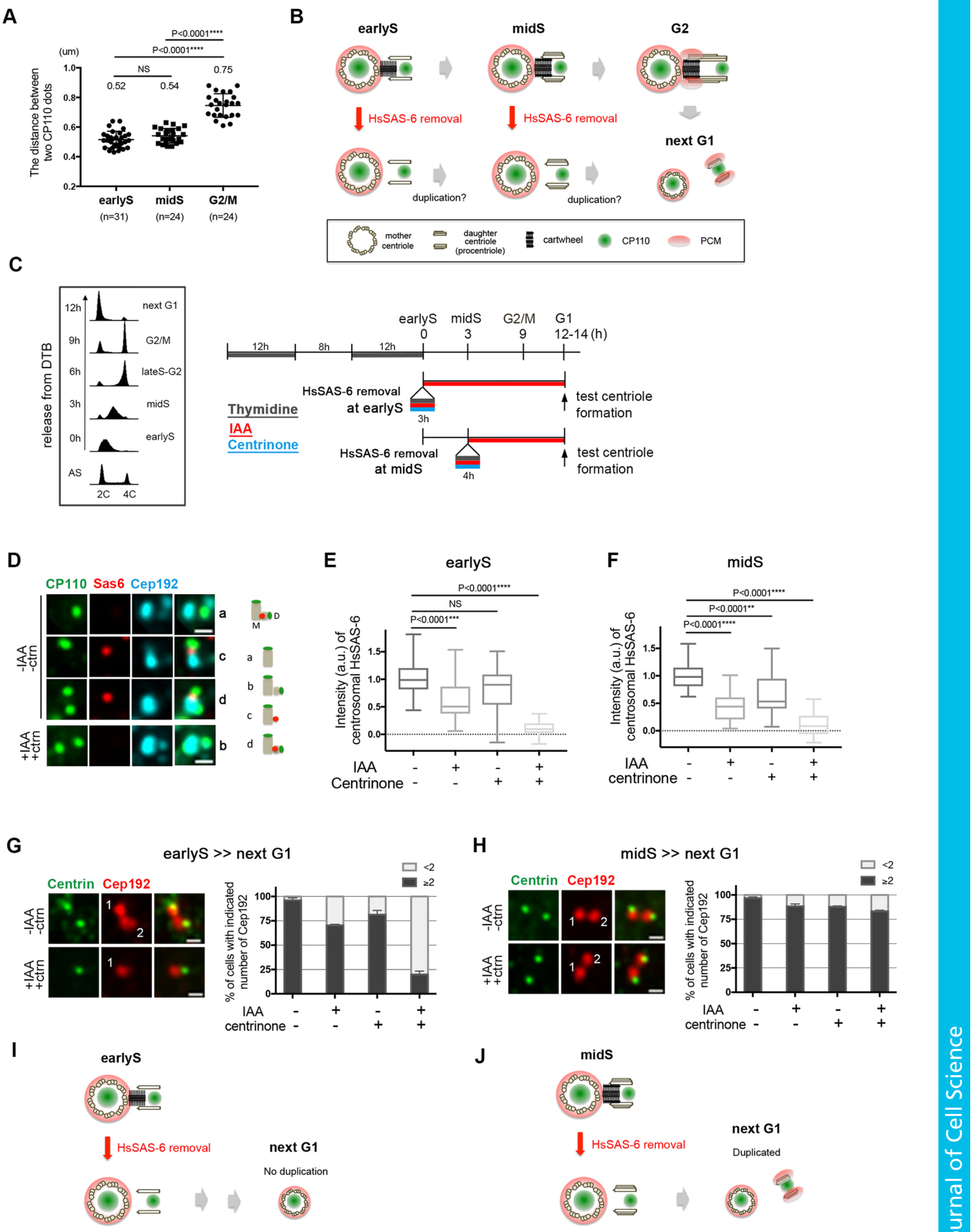

Fig. 4. See next page for legend.

Fig. 4. HsSAS-6-AID removal from the centriole in the middle of procentriole formation. (A) The length of procentrioles was monitored by measuring the distance between two CP110 dots at the mother and daughter centrioles. Each number above the plot indicates the mean distance. Error bars indicate the s.d. ****P<0.0001; NS, not significantly different (P>0.05) (one-way ANOVA). (B) Schematic illustration of what occurs after cartwheel removal in the HsSAS-6-AID cell line in the middle of procentriole formation. (C) Experimental scheme of HsSAS-6 removal from centrioles in S-phase arrested cells. Cells were synchronized at G1/S border (early S phase) by DTB (2 mM thymidine for 12 h, release for 8 h and thymidine for 12 h). For HsSAS-6-AID removal in the early S phase, cells were treated with 0.5 mM IAA and/or 100 nM centrinone for 3 h, and released into fresh medium with IAA until next G1. For HsSAS-6-AID removal in the middle S phase, cells were released once for 3 h and arrested with thymidine, again with IAA and/or centrinone, for 4 h, and released into fresh medium with IAA until the next G1. Cell cycle progression was monitored by flow cytometry (left and Fig. S3F). (D) Representative patterns of CP110 and HsSAS-6 after the drug treatment. Patterns are classified into one of four catergories; a, one CP110 dot without HsSAS-6; b, two CP110 dots without HsSAS-6; c, one CP110 dot with HsSAS-6; d, two CP110 dots with HsSAS-6. Quantifications are shown in Fig. S3G. (E,F) The signal intensities of centosomal HsSAS-6 after IAA and/or centrinone treatment were quantified in the early S (E) and in the middle S (F), respectively. Cytoplasmic HsSAS-6 signals were subtracted from centrosomal HsSAS-6 signals in each cell. Total counts from two independent experiments are shown (n=33, 30, 26, 29 in c; n=24, 18, 19, 23 in d, for each condition, respectively). ****P<0.0001; ns, not significantly different (P>0.05) (one-way ANOVA). The box represents the 25–75th percentiles, and the median is indicated. The whiskers show the range of centrosomal HsSAS-6 signal intensities. (G,H) Representative patterns of Cep192 foci in the next G1 phase after HsSAS-6 removal in the early S phase (G) or middle S phase (H) are shown. Numbers in the Cep192 staining images represent the counting of mature centrioles. Right, the number of centrioles, as determined by the counting of mature Cep192 puncta, was quantified according to the patterns shown in Fig. S3E. Values are mean±s.e.m. percentages from three independent experiments (n≥35 for each condition). (I,J) Schematic illustration for the consequences of HsSAS-6 removal at early S phase (I) and mid S phase (J) in procentriole formation.

In the early S phase, Cep295 was already detectable at the procentriole assembly site in most centrosomes, and acetylation of centriolar microtubules also could also be seen; however, Cep135 and Cep192 had not yet been loaded (Fig. S4A,C,D). As centriole formation proceeded during the S phase, the border of Cep295 signals between the mother centriole and procentriole became clearer, and interestingly, loading of Cep135 to procentriole assembly sites was frequently observed (Fig. S4A,B). The recruitment of Cep192 at the walls of the procentrioles was frequently detectable only during the late S and G2 phases (Fig. S4A).

A recent study using cell-free cartwheel reconstitution with *C. reinhardtii* (Cr)SAS-6 revealed that Cep135/Bld10 is required for well-organized stacking of cartwheels (Guichard et al., 2017). Our data support the idea that that Cep135 loading may be a key event for stabilizing the procentriole structure (Fig. S4E). Overall, our results experimentally demonstrated for the first time the importance of HsSAS-6 until the procentriole structure is stabilized for subsequent maturation.

Another role of the cartwheel for restricting the procentriole assembly site

We next focused on the localization of Plk4 and STIL at the centrioles upon HsSAS-6 removal. The phosphorylation of STIL by Plk4 has been shown to facilitate STIL–HsSAS-6 interaction and centriolar loading of HsSAS-6, which drives negative regulation to ensure that only a single duplication site is initiated for each mother centriole (Ohta et al., 2014, 2018). Interestingly, a previous study showed that after AID-mediated Plk4 destruction or Plk4 inactivation with an analog-sensitive mutant ($Plk4^{AS}$), STIL rapidly disappeared from the centriole whereas HsSAS-6 was retained (Kim et al., 2016; Lambrus et al., 2015). This suggests that once the cartwheel structure is assembled, the interaction between HsSAS-6 and Plk4–STIL might be dispensable for the maintenance of the cartwheel structure.

Hence, we tested the behavior of Plk4 and STIL after HsSAS-6 removal from the centriole in the HsSAS-6-AID cell line. Interestingly, after 6 h of IAA treatment during the S and G2 phases, the intensities of HsSAS-6 and STIL at the centriole were similarly decreased, with only a slight difference [83% decreased (Fig. 5A,B,D,G) and 59% decreased (Fig. 5A,B,E,G) for HsSAS-6 and STIL, respectively]. By contrast, the intensity of Plk4 was increased more than twofold and returned to the ring-like pattern that is normally seen around the mother centriole wall during G1 and prior to procentriole formation (Fig. 5C,F,H). These results suggest that HsSAS-6 is required for restricting the presence of the Plk4–STIL module only at the procentriole assembly site, presumably to suppress the formation of additional centrioles after the intermediate structure is assembled (Fig. 5I).

DISCUSSION

In this study, we demonstrated human SAS-6 self-assembly *in vitro* and established that the ability of SAS-6 to assemble in the central part of the cartwheel structure is conserved. We also characterized the function of the cartwheel in centriole formation by developing a system for inducible HsSAS-6 degradation in human cells. We demonstrated that HsSAS-6 is essential not only for the initiation of procentriole formation, but also for the stabilization of the proximal half of the procentriole (Fig. 5J). However, it seems that the cartwheel structure is dispensable for the subsequent steps of full elongation and maturation of centrioles. Such requirement of the cartwheel structure implies a stepwise procentriole assembly in the following way. First, several layers of cartwheel structures are stacked on the mother centriole wall to establish the overall geometry of a procentriole. At this stage, the procentriole assembly is already limited to one site, while the centriole intermediate still requires the cartwheel structures for its maintenance. Thereafter, some critical components, such as Cep295 and Cep135, are incorporated into the intermediate (Fig. S4A–C,E), presumably in a cartwheel-dependent manner, and these would be expected to facilitate arrangement of centriolar triplet microtubules and further procentriole elongation. This step could ensure the stability of the centriole intermediate, thus serving as a critical transition point for the necessity of the cartwheel structure, as a scaffold (Fig. 5J). In *Chlamydomonas*, Bld10p/Cep135 is known to be an essential protein for cartwheel assembly by interacting with SAS-6 at its C-terminus and connecting the central hub with triplet microtubules. However, in humans, how Cep135 is involved in the procentriole assembly is not fully understood. In our previous study, we showed that Cep295 is required for the recruitment of Cep135 to the daughter centriole. Together with the findings in this study, it is possible that the acquisition of Cep135 leads to the stabilization of the centriole intermediate, and it would allow further elongation and maturation of the procentriole.

Additionally, our data suggest a novel function of HsSAS-6 at procentrioles. Given the observation that the depletion of HsSAS-6 after procentriole formation led to a significant increase in Plk4 around the mother centriole wall, the existence of an intact cartwheel structure is presumably necessary to maintain the system and suppress the formation of extra procentrioles (Fig. 5I,J). It would be interesting to clarify how the structural integrity of the cartwheel is monitored, and how such information is transmitted, so as to block centriolar accumulation of Plk4 and the formation of extra procentrioles. Our

Journal of Cell Science (2019) 132, jcs217521. doi:10.1242/jcs.217521

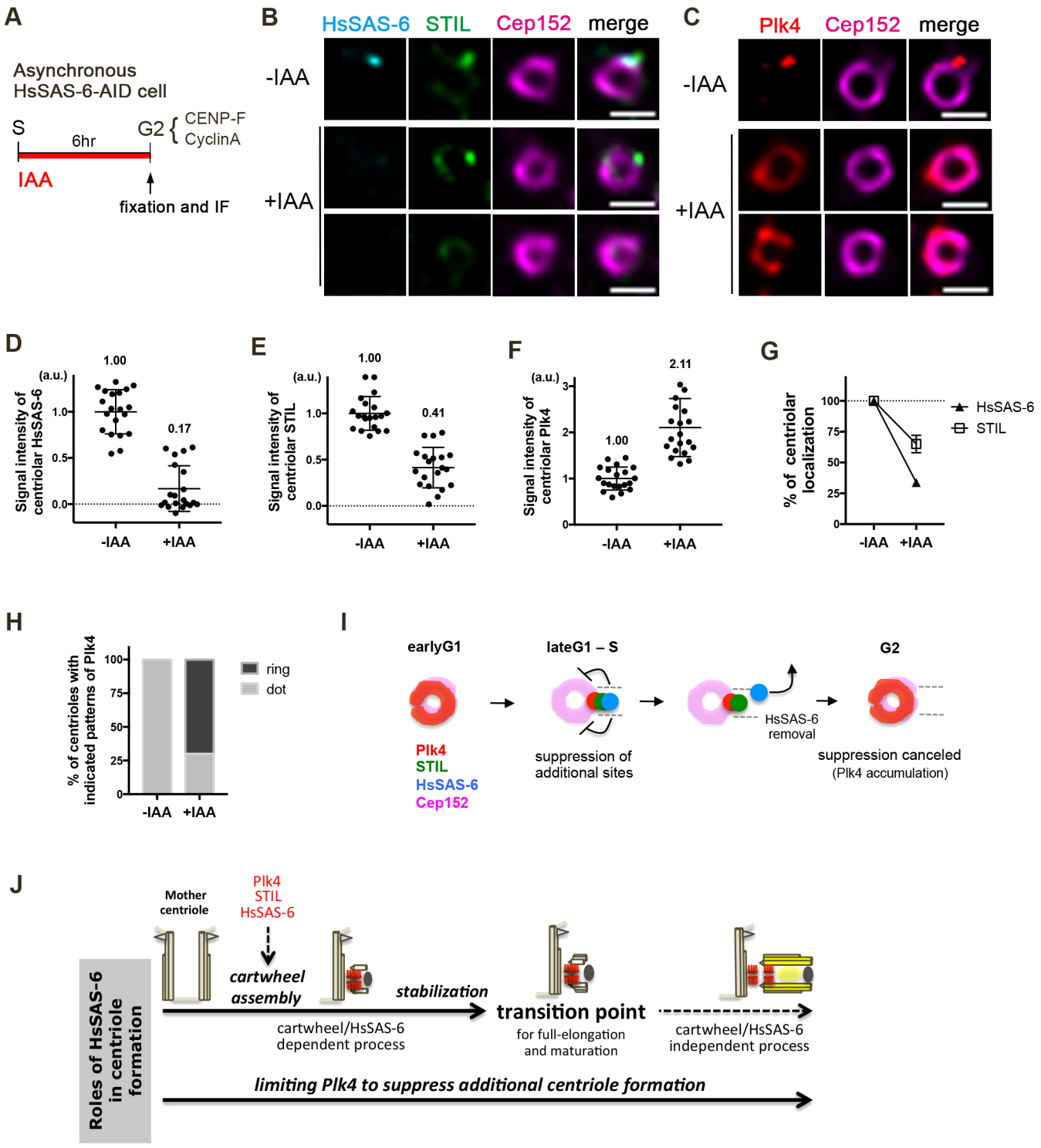

Fig. 5. See next page for legend.

approach of using transient degradation of HsSAS-6 might provide insight into this as-yet-unexplored mechanism.

MATERIALS AND METHODS

Cell culture, cell cycle synchronization and flow cytometry

U2OS cells were obtained from the European Collection of Cell Culture (ECACC). Cells were cultured in Dulbecco's modified Eagle's medium (DMEM) supplemented with 10% fetal bovine serum at 37°C in 5% CO_2. HCT116 cells were cultured in McCoy's 5A medium supplemented with 10% fetal bovine serum and 2 mM L-glutamine. All cell lines were tested and shown to be without mycoplasma contamination.

To synchronize HCT116 cells at prometaphase, cells were treated with 100 ng/ml nocodazole for 12 h, washed three times with PBS and released into fresh medium. For cell synchronization in the early S phase, cells were treated with 2 mM thymidine for 12 h, released 8 h and treated with thymidine for 12 h again (double thymidine block; DTB).

To induce degradation of HsSAS-6–AID, 0.5 mM indole-3-acetic acid (IAA) was added to the culture medium. For HsSAS-6–AID removal

Fig. 5. A further role of HsSAS-6 for restricting the procentriole assembly site. (A) Experimental scheme of HsSAS-6 removal in the middle of centriole formation in asynchronous HsSAS-6-AID cell line. Cells were treated with 0.5 mM IAA for 6 h, and fixed and analyzed in the G2 phase. Centrioles in the G2 phase were distinguished through CENP-F or cyclin A staining (data not shown). (B,C) Representative patterns of HsSAS-6 and STIL (B) and Plk4 (C) staining at the centrioles after IAA treatment are shown. Images were taken with a Leica TCS SP8 Hyvolution system. Scale bars: 500 nm. Note that Plk4 turned out to show a ring-like pattern around the mother centriole wall after IAA treatment. (D–F) Signal intensities (a.u., arbitrary units) of HsSAS-6 (D), STIL (E) and Plk4 (F) at centrioles after IAA treatment were quantified. Each number above the plot indicates the mean values of 20 samples from two independent experiments. Error bars indicate the s.d. (G) Percentages of centriolar localization of HsSAS-6 and STIL after IAA treatment are shown. Error bars indicate the s.d. Values are mean percentages from two independent experiments (n=20 total cells analyzed). (H) The percentages of centrioles with a dot or ring-like pattern for Plk4 were quantified. Total counts (n=20) are from two independent experiments in each condition. (I) Schematic summary of the phenotypes of HsSAS-6 removal after procentriole formation, and how HsSAS-6 maintains the negative regulation to restrict the daughter centriole assembly to one site per each mother centriole. (J) Hypothetical model for the role of HsSAS-6/the cartwheel structure in the initiation of centriole formation to the transition point, and in monitoring the integrity of growing procentriole and the procentriole number. The assembly of cartwheel structure initiates procentriole formation. The cartwheel structure acts as a scaffold to assemble a procentriole intermediate until Cep295 and Cep135 are sequentially loaded to the procentriole assembly site. After this transition point, the structural integrity of the intermediate is ensured, even without the cartwheel structure, for further elongation and maturation. The transition point may be associated with a stack of cartwheel structures and establishment of centriolar triplet-microtubules. HsSAS-6 is also potentially necessary for suppressing the formation of additional procentrioles by limiting active Plk4 to only a single procentriole assembly site.

in the S phase-arrested cells, they were treated with 0.5 mM IAA and/or 100 nM centrinone.

For flow cytometry analysis, cells were harvested and fixed in 70% ethanol. Fixed cells were washed and resuspended in PBS containing 1% BSA, 50 µg/ml RNaseA and 40 µg/ml propidium iodide. Then cells were incubated at 37°C for 30 min, filtered through a nylon mesh filter and analyzed by the Accuri C6 FACS machine (BD) equipped with FCS4 Express Cytometry software (De Novo Software).

Gene targeting

The HsSAS-6-AID cell line was generated in the HCT116 CMV-OsTIR1 cell line (RIKEN BRC, RCB4662) by using the CRISPR/Cas9 system, as previously described (Natsume et al., 2016; Ran et al., 2013). GuideRNA oligonucleotides were hybridized and cloned into the BbsI-digested pX330 (Addgene #42230). To generate the homology-directed repair (HDR) targeting plasmids, a 500 bp synthetic target genomic DNA in modified pUC57 (GENEWIZ) was digested by BamHI, and an AID tag with a hygromycin or neomycin resistance cassette was cloned into the site. Genome information was obtained from NCBI RefSeq (NG_051914.1). Oligonucleotides and synthetic DNA sequences used here are listed in Table S1. Plasmids were generated using PrimeSTAR MAX DNA polymerase and/or the In-Fusion cloning system (TaKaRa). Transfection and colony selection were performed as previously described (Natsume et al., 2016).

Genomic PCR and mRNA detection

To prepare genomic DNA, cells were lysed in 50 mM NaOH solution, boiled and neutralized with 100 mM Tris-HCl pH 8.0. The lysate was briefly spun down and the supernatant was served as a template. Genomic PCR was carried out using Phire Hot Start ll DNA polymerase (Thermo Fisher Scientific), according to the manufacturer's instructions. The following primers were used in this study: a, 5′-ATCTTCCAAACCCACAGCGC-3′; b, 5′-TTCTTGACGAGTTCTTCTGA-3′; c, 5′-GCCAAGTTCTAATTCCATCAG-3′; and d, 5′-TTTACCAATCCCCAAGTACA-3′.

For the detection of mRNA, total RNA was prepared with TRIzol Reagent (Life Technologies). Reverse transcription and following DNA amplification were performed by using a One Step PrimeScript RT-PCR Kit (TaKaRa). For each sample, 10 ng of total RNA was served as a template for semi-quantitative RT-PCR. The following primers were used in this study: *Hprt_fw*, 5′-GCAGACTTTGCTTTCCTTGG-3′ and *Hprt_rv*, 5′-CTCCAGATGTTTCCAAACTCAA-3′; *HsSAS-6_ex14_fw*, 5′-GTTGATGGTAGACTGACTTA-3′ and *HsSAS-6_ex15_rv*, 5′-TTTTCCTTATCAGTTG-AGCA-3′. The following siRNAs were used (Life Technologies): Silencer Select siRNA against HsSAS-6 ORF (s46487), negative control #1 (4390843).

Antibodies

The following primary antibodies were used in this study: mouse monoclonal antibodies against Plk4 [Merck Millipore, 6H5, MABC544, for immunofluorescence (IF) 1:250], HsSAS-6 (Santa Cruz Biotechnology, sc-81431, IF 1:250), centrin-1 (Millipore, 20H5, IF 1:500), centrobin (Abcam, ab70448, IF 1:1000), γ-tubulin (GTU88) (Sigma, T5192, IF 1:1000), polyglutamylation modification (GT335, mAb) (AdipoGen, AG-20B-0020-C100, IF 1:1000), mAID (MBL, IF 1:500), NEDD1 (Abcam, ab57336, IF 1:1000) and Cyclin A (Abcam, 6E6, ab16726, IF 1:1000); and rabbit polyclonal antibodies against HsSAS-6 [Santa Cruz Biotechnology, sc-98506, for western blotting (WB) 1:2000], Cep295/KIAA1731 (Sigma-Aldrich, HPA038596, IF 1:1000), Cep192 (a gift from Laurence Pelletier, Lunenfeld-Tanenbaum Research Institute, Department of Molecular Genetics, University of Toronto, Canada, IF 1:1000), Cep192 (Bethyl, A302-324A, IF 1:1000), Cep152 (Bethyl, A302-479A and A302-480A, IF 1:1000), CP110 (proteintech, 12780-1-AP, IF 1:500), hPoc5 (Bethyl, A303-341A, IF 1:1000), STIL (Abcam, ab89314, IF 1:250, WB 1:2000) and CENP-F (Bethyl A301-617A, IF 1:1000). Secondary antibodies used were conjugated to Alexa Fluor 488, 568, 555, 594 and 647 (Molecular Probes, IF 1:1000). Alexa Fluor 488 or 647-labeled Cep192 and Cep152 were generated with Alexa Fluor labeling kits (Life Technologies) and used for triple staining (IF 1:500). Hoechest 33258 (Dojindo, IF 2 mg/ml) was used for nuclear staining. Goat polyclonal antibodies against mouse IgG (Promega, W402B, 1:5 000) and rabbit IgG (Promega, W401B, 1:5000) conjugated to horseradish peroxidase were used for western blotting.

Immunofluorescence

For immunofluorescence analysis, cells were cultured on the coverslips, fixed with ice-cold methanol for 5 min at 20°C and washed with PBS. Then cells were permealized with 0.05% Triton X-100 in PBS (PBST), and incubated with primary antibodies in 3% BSA in PBST overnight at 4°C. After cells were washed with PBST twice, they were incubated with secondary antibodies for 1 h at room temperature. For triple staining with Alexa Fluor-labeled antibodies, cells were treated after secondary antibodies were washed out. Then cells were stained with Hoechst 33258 for 5 min, washed with PBST again and mounted onto the glass slides for observation.

Immunoprecipitation and western blotting

For preparation of total cell lysates, cells were washed with PBS, lysed in lysis buffer [20 mM Tris-HCl pH 7.5, 150 mM NaCl, 0.5% Triton X-100, 1 mM DTT, 2 mM $MgCl_2$ and 1:1000 protease inhibitor cocktail (Nacalai Tesque)] and insoluble material was removed by centrifugation (15,000 ***g*** for 20 min). SDS-PAGE was performed using 6–12% polyacrylamide gels, followed by transfer on Immobilon-P membrane (Millipore Corporation). The membrane was probed with the primary antibodies, washed with 0.02% Tween 20 in PBS and incubated with HRP-conjugated secondary antibodies. The signals were detected with ECL Prime/Select reagents (GE healthcare) via the Chemi Doc XRSþ system (Bio-Rad).

Microscopy and super-resolution microscopy

The number of fluorescence signals were observed and counted from images acquired with an Axioplan2 fluorescence microscope (Carl Zeiss) with a 100×/1.4 NA plan-APOCHROMAT objective lens. Image capture and the signal quantification were performed using a DeltaVision deconvolution microscope (GE Healthcare) with softWoRx software (Applied Precision). For quantification of centriole signals, the values of the intensities were obtained from 'Data Inspector' in Tools in softWoRx. The values of cytoplasmic signals were subtracted from those of centriole signals. The

reminder after the subtraction was taken as the value of centriole signal, and analyzed for statistical significance.

To obtain high-resolution images, the Leica TCS SP8 Hyvolution system with Huygens essential software (Scientific Volume Imaging; SVI) was used. The parameters of the settings were as previously described (Tsuchiya et al., 2016).

STED mages were taken with a Leica TCS SP8 STED system with a Leica HC PL APO 100×/1.40 oil STED WHITE objective, and 660 nm gated STED. The scan speed was set to 100 Hz in combination with five fold line average in a 512×80 format (pixel size 15 or 20 nm). The images were collected at 180 nm *z* steps. The STED images were processed by deconvolution with Huygens professional software (SVI). For the projection of *Z* images, max projection was applied by ImageJ. In this study, we visualized proteins of interest via Alexa Fluor 555-conjugated antibodies whereas the marker proteins were visualized by using Alexa Fluor 488-conjugated antibodies. Each pattern was tested at least in five cells from two independent experiments.

In vitro reconstitution with lipid monolayer

The GST–HsSAS-6 NL fragment was expressed in *E. coli* and purified by using glutathione–Sepharose beads (GE 17075601). The GST tag was cleaved by treatment with prescission protease (GE 27084301) and removed. The cleaved sample was gel-filtrated with Superdex 200 10/300 GL column (GE Healthcare), and assessed by SDS-PAGE and Simply Blue Safe staining. For *in vitro* reconstitution on lipid monolayer, used a modified version of the 'Lipid Monolayer Assay Protocol' from the Harvey McMahon laboratory website (http://www2.mrc-lmb.cam.ac.uk/groups/hmm/techniqs/mono.html). A lipid mixture containing 10% cholesterol, 40% phosphatidylehanolamine (PE), 40% phosphatidylcholine (PC) and 10% phosphatidylserine (PS) to a final concentration of 0.1 mg/ml in chloroform was loaded on the chamber filled with HKM buffer (25 mM Hepes pH7.4, 125 mM potassium acetate, 5 mM magnesium acetate, 1 mM dithiothreitol), and incubated for 1 h at room temperature to form a lipid monolayer. Then an electron microscopy (EM) grid was set on the layer, and protein solution was applied and incubated for 3 h at room temperature for the assembly of protein complex on the lipid monolayer. The sample was stained with 2% uranyl acetate and observed with a transmission electron microscope JEM-1010 (JEOL). Images were acquired by a VELETA CCD camera and analyzed with iTEM software (SEIKA Corporation).

Statistical analysis

Statistical analyses were performed using GraphPad Prism software (version 7.0) and Microsoft Excel. Comparisons between two groups were performed with a two-tailed *t*-test and comparisons among groups were performed by one-way ANOVA. Statistical significance was assigned for $P<0.05$, unless otherwise mentioned in the text.

Acknowledgements

We are grateful to Rie Hayashi at Leica Microsystems for technical support and access to STED microscopy facilities. We thank Andrew Shiau and Karen Oegema at the Ludwig Institute for Cancer Research for providing the PLK4 inhibitor centrinone, Harvey McMahon at MRC Laboratory of Molecular Biology for kindly giving us a Teflon block for the lipid monolayer assay, and Kazuko Ohishi for technical assistance. We also thank Kitagawa lab members for critical reading of the manuscript and advice on the experiments.

Competing interests

The authors declare no competing or financial interests.

Author contributions

Conceptualization: S.Y., D.K.; Methodology: S.Y.; Validation: S.Y.; Formal analysis: S.Y.; Investigation: S.Y., Y.T., M.O., A.G., G.S., Y.N., T.A.; Resources: T.F., T.N., M.T.K.; Writing - original draft: S.Y.; Writing - review & editing: S.Y., D.K.; Visualization: S.Y.; Supervision: D.K.; Project administration: S.Y., D.K.; Funding acquisition: S.Y., D.K.

Funding

This work was supported by Grant-in-Aid for Japan Society for the Promotion of Science (JSPS) Fellows, for Young Scientists (A) (16H06168), for Young Scientists (B) (16K18541) and for Scientific Research on Innovative Areas from the Ministry of Education, Culture, Sports, Science and Technology of Japan (24113003), by Takeda Science Foundation, by Daiichi Sankyo foundation of Life Science, by NOVARTIS Foundation (Japan) for the Promotion of Science, and by Uehara Memorial Foundation.

Supplementary information

Supplementary information available online at
http://jcs.biologists.org/lookup/doi/10.1242/jcs.217521.supplemental

References

Arquint, C. and Nigg, E. A. (2014). STIL microcephaly mutations interfere with APC/C-mediated degradation and cause centriole amplification. *Curr. Biol.* **24**, 351-360. doi:10.1016/j.cub.2013.12.016

Arquint, C., Gabryjonczyk, A.-M., Imseng, S., Böhm, R., Sauer, E., Hiller, S., Nigg, E. A. and Maier, T. (2015). STIL binding to Polo-box 3 of PLK4 regulates centriole duplication. *eLife* **4**, e07888. doi:10.7554/eLife.07888

Azimzadeh, J., Hergert, P., Delouvée, A., Euteneuer, U., Formstecher, E., Khodjakov, A. and Bornens, M. (2009). hPOC5 is a centrin-binding protein required for assembly of full-length centrioles. *J. Cell Biol.* **185**, 101-114. doi:10.1083/jcb.200808082

Brito, D. A., Gouveia, S. M. and Bettencourt-Dias, M. (2012). Deconstructing the centriole: structure and number control. *Curr. Opin. Cell Biol.* **24**, 4-13. doi:10.1016/j.ceb.2012.01.003

Chang, C.-W., Hsu, W.-B., Tsai, J.-J., Tang, C.-J. C. and Tang, T. K. (2016). CEP295 interacts with microtubules and is required for centriole elongation. *J. Cell Sci.* **129**, 2501-2513. doi:10.1242/jcs.186338

Chiu, W. (1997). Electron crystallography of macromolecular periodic arrays on phospholipid monolayers. *Adv. Biophys.* **34**, 161-172. doi:10.1016/S0065-227X(97)89638-4

Culver, B. P., Meehl, J. B., Giddings, T. H. and Winey, M. (2009). The two SAS-6 homologs in Tetrahymena thermophila have distinct functions in basal body assembly. *Mol. Biol. Cell* **20**, 1865-1877. doi:10.1091/mbc.e08-08-0838

Dammermann, A., Müller-Reichert, T., Pelletier, L., Habermann, B., Desai, A. and Oegema, K. (2004). Centriole assembly requires both centriolar and pericentriolar material proteins. *Dev. Cell* **7**, 815-829. doi:10.1016/j.devcel.2004.10.015

Dzhindzhev, N. S., Tzolovsky, G., Lipinszki, Z., Schneider, S., Lattao, R., Fu, J., Debski, J., Dadlez, M. and Glover, D. M. (2014). Plk4 phosphorylates ana2 to trigger SAS6 recruitment and procentriole formation. *Curr. Biol.* **24**, 2526-2532. doi:10.1016/j.cub.2014.08.061

Fong, C. S., Kim, M., Yang, T. T., Liao, J.-C. and Tsou, M.-F. B. (2014). SAS-6 assembly templated by the lumen of cartwheel-less centrioles precedes centriole duplication. *Dev. Cell* **30**, 238-245. doi:10.1016/j.devcel.2014.05.008

Ford, M. G. J., Pearse, B. M., Higgins, M. K., Vallis, Y., Owen, D. J., Gibson, A., Hopkins, C. R., Evans, P. R. and McMahon, H. T. (2001). Simultaneous binding of PtdIns(4,5)P2 and clathrin by AP180 in the nucleation of clathrin lattices on membranes. *Science* **291**, 1051-1055. doi:10.1126/science.291.5506.1051

Ford, M. G. J., Mills, I. G., Peter, B. J., Vallis, Y., Praefcke, G. J. K., Evans, P. R. and McMahon, H. T. (2002). Curvature of clathrin-coated pits driven by epsin. *Nature* **419**, 361-366. doi:10.1038/nature01020

Fu, J., Hagan, I. M. and Glover, D. M. (2015). The centrosome and its duplication cycle. *Cold Spring Harb. Perspect. Biol.* **7**, a015800. doi:10.1101/cshperspect.a015800

Fu, J., Lipinszki, Z., Rangone, H., Min, M., Mykura, C., Chao-Chu, J., Schneider, S., Dzhindzhev, N. S., Gottardo, M., Riparbelli, M. G. et al. (2016). Conserved molecular interactions in centriole-to-centrosome conversion. *Nat. Cell Biol.* **18**, 87-99. doi:10.1038/ncb3274

Godinho, S. A. and Pellman, D. (2014). Causes and consequences of centrosome abnormalities in cancer. *Philos. Trans. R. Soc. Lond. B. Biol. Sci.* **369**, 1650. doi:10.1098/rstb.2013.0467

Gönczy, P. (2012). Towards a molecular architecture of centriole assembly. *Nat. Rev. Mol. Cell Biol.* **13**, 425-435. doi:10.1038/nrm3373

Guichard, P., Chrétien, D., Marco, S. and Tassin, A.-M. (2010). Procentriole assembly revealed by cryo-electron tomography. *EMBO J.* **29**, 1565-1572. doi:10.1038/emboj.2010.45

Guichard, P., Desfosses, A., Maheshwari, A., Hachet, V., Dietrich, C., Brune, A., Ishikawa, T., Sachse, C. and Gonczy, P. (2012). Cartwheel architecture of trichonympha basal body. *Science* **337**, 553-553. doi:10.1126/science.1222789

Guichard, P., Hamel, V., Le Guennec, M., Banterle, N., Iacovache, I., Nemčíková, V., Flückiger, I., Goldie, K. N., Stahlberg, H., Lévy, D. et al. (2017). Cell-free reconstitution reveals centriole cartwheel assembly mechanisms. *Nat. Commun.* **8**, 14813. doi:10.1038/ncomms14813

Hilbert, M., Noga, A., Frey, D., Hamel, V., Guichard, P., Kraatz, S. H. W., Pfreundschuh, M., Hosner, S., Flückiger, I., Jaussi, R., et al. (2016). SAS-6 engineering reveals interdependence between cartwheel and microtubules in determining centriole architecture. *Nat. Cell Biol.* **18**, 393-403. doi:10.1038/ncb3329

Keller, D., Orpinell, M., Olivier, N., Wachsmuth, M., Mahen, R., Wyss, R., Hachet, V., Ellenberg, J., Manley, S. and Gönczy, P. (2014). Mechanisms of HsSAS-6

assembly promoting centriole formation in human cells. *J. Cell Biol.* **204**, 697-712. doi:10.1083/jcb.201307049

Kilburn, C. L., Pearson, C. G., Romijn, E. P., Meehl, J. B., Giddings, T. H., Culver, B. P., Yates, J. R. and Winey, M. (2007). New Tetrahymena basal body protein components identify basal body domain structure. *J. Cell Biol.* **178**, 905-912. doi:10.1083/jcb.200703109

Kim, M., O'Rourke, B. P., Soni, R. K., Jallepalli, P. V., Hendrickson, R. C. and Tsou, M.-F. B. (2016). Promotion and suppression of centriole duplication are catalytically coupled through PLK4 to ensure centriole homeostasis. *Cell Rep.* **16**, 1-9. doi:10.1016/j.celrep.2016.06.069

Kitagawa, D., Vakonakis, I., Olieric, N., Hilbert, M., Keller, D., Olieric, V., Bortfeld, M., Erat, M. C., Flückiger, I., Gönczy, P. et al. (2011). Structural basis of the 9-fold symmetry of centrioles. *Cell* **144**, 364-375. doi:10.1016/j.cell.2011.01.008

Kratz, A.-S., Bärenz, F., Richter, K. T. and Hoffmann, I. (2015). Plk4-dependent phosphorylation of STIL is required for centriole duplication. *Biol. Open* **4**, 370-377. doi:10.1242/bio.201411023

Lambrus, B. G., Uetake, Y., Clutario, K. M., Daggubati, V., Snyder, M., Sluder, G. and Holland, A. J. (2015). p53 protects against genome instability following centriole duplication failure. *J. Cell Biol.* **210**, 63-77. doi:10.1083/jcb.201502089

Leidel, S., Delattre, M., Cerutti, L., Baumer, K. and Gönczy, P. (2005). SAS-6 defines a protein family required for centrosome duplication in C. elegans and in human cells. *Nat. Cell Biol.* **7**, 115-125. doi:10.1038/ncb1220

Lévy, D., Mosser, G., Lambert, O., Moeck, G. S., Bald, D. and Rigaud, J.-L. (1999). Two-dimensional crystallization on lipid layer: a successful approach for membrane proteins. *J. Struct. Biol.* **127**, 44-52. doi:10.1006/jsbi.1999.4155

Lin, Y.-C., Chang, C.-W., Hsu, W.-B., Tang, C.-J. C., Lin, Y.-N., Chou, E.-J., Wu, C.-T. and Tang, T. K. (2013). Human microcephaly protein CEP135 binds to hSAS-6 and CPAP, and is required for centriole assembly. *EMBO J.* **32**, 1141-1154. doi:10.1038/emboj.2013.56

Matsuura, K., Lefebvre, P. A., Kamiya, R. and Hirono, M. (2004). Bld10p, a novel protein essential for basal body assembly in Chlamydomonas: localization to the cartwheel, the first ninefold symmetrical structure appearing during assembly. *J. Cell Biol.* **165**, 663-671. doi:10.1083/jcb.200402022

Moyer, T. C., Clutario, K. M., Lambrus, B. G., Daggubati, V. and Holland, A. J. (2015). Binding of STIL to Plk4 activates kinase activity to promote centriole assembly. *J. Cell Biol.* **209**, 863-878. doi:10.1083/jcb.201502088

Nakazawa, Y., Hiraki, M., Kamiya, R. and Hirono, M. (2007). SAS-6 is a cartwheel protein that establishes the 9-fold symmetry of the centriole. *Curr. Biol.* **17**, 2169-2174. doi:10.1016/j.cub.2007.11.046

Natsume, T., Kiyomitsu, T., Saga, Y. and Kanemaki, M. T. (2016). Rapid protein depletion in human cells by auxin-inducible degron tagging with short homology donors. *Cell Rep.* **15**, 210-218. doi:10.1016/j.celrep.2016.03.001

Nigg, E. A. and Raff, J. W. (2009). Centrioles, centrosomes, and cilia in health and disease. *Cell* **139**, 663-678. doi:10.1016/j.cell.2009.10.036

Nishimura, K., Fukagawa, T., Takisawa, H., Kakimoto, T. and Kanemaki, M. (2009). An auxin-based degron system for the rapid depletion of proteins in nonplant cells. *Nat. Methods* **6**, 917-922. doi:10.1038/nmeth.1401

Ohta, M., Ashikawa, T., Nozaki, Y., Kozuka-Hata, H., Goto, H., Inagaki, M., Oyama, M. and Kitagawa, D. (2014). Direct interaction of Plk4 with STIL ensures formation of a single procentriole per parental centriole. *Nat. Commun.* **5**, 5267. doi:10.1038/ncomms6267

Ohta, M., Watanabe, K., Ashikawa, T., Nozaki, Y., Yoshiba, S., Kimura, A. and Kitagawa, D. (2018). Bimodal binding of STIL to Plk4 controls proper centriole copy number. *Cell Rep.* **23**, 3160-3169.e4. doi:10.1016/j.celrep.2018.05.030

Qiao, R., Cabral, G., Lettman, M. M., Dammermann, A. and Dong, G. (2012). SAS-6 coiled-coil structure and interaction with SAS-5 suggest a regulatory mechanism in C. elegans centriole assembly. *EMBO J.* **31**, 4334-4347. doi:10.1038/emboj.2012.280

Ran, F. A., Hsu, P. D., Wright, J. and Agarwala, V. (2013). Genome engineering using the CRISPR-Cas9 system. *Nat. Protoc.* **8**, 2281-2308. doi:10.1038/nprot.2013.143

Rodrigues-Martins, A., Bettencourt-Dias, M., Riparbelli, M., Ferreira, C., Ferreira, I., Callaini, G. and Glover, D. M. (2007). DSAS-6 organizes a tube-like centriole precursor, and its absence suggests modularity in centriole assembly. *Curr. Biol.* **17**, 1465-1472. doi:10.1016/j.cub.2007.07.034

Saurya, S., Roque, H., Novak, Z. A., Wainman, A., Aydogan, M. G., Volanakis, A., Sieber, B., Pinto, D. M. S. and Raff, J. W. (2016). *Drosophila* Ana1 is required for centrosome assembly and centriole elongation. *J. Cell Sci.* **129**, 2514-2525. doi:10.1242/jcs.186460

Stevens, N. R., Roque, H. and Raff, J. W. (2010). DSas-6 and Ana2 coassemble into tubules to promote centriole duplication and engagement. *Dev. Cell* **19**, 913-919. doi:10.1016/j.devcel.2010.11.010

Strnad, P., Leidel, S., Vinogradova, T., Euteneuer, U., Khodjakov, A. and Gönczy, P. (2007). Regulated HsSAS-6 levels ensure formation of a single procentriole per centriole during the centrosome duplication cycle. *Dev. Cell* **13**, 203-213. doi:10.1016/j.devcel.2007.07.004

Tsuchiya, Y., Yoshiba, S., Gupta, A., Watanabe, K. and Kitagawa, D. (2016). Cep295 is a conserved scaffold protein required for generation of a bona fide mother centriole. *Nat. Commun.* **7**, 12567. doi:10.1038/ncomms12567

van Breugel, M., Hirono, M., Andreeva, A., Yanagisawa, H., Yamaguchi, S., Nakazawa, Y., Morgner, N., Petrovich, M., Ebong, I.-O., Robinson, C. V. et al. (2011). Structures of SAS-6 suggest its organization in centrioles. *Science* **331**, 1196-1199. doi:10.1126/science.1199325

van Breugel, M., Wilcken, R., McLaughlin, S. H., Rutherford, T. J. and Johnson, C. M. (2014). Structure of the SAS-6 cartwheel hub from Leishmania major. *eLife* **3**, e01812. doi:10.7554/eLife.01812

Wong, Y. L., Anzola, J. V., Davis, R. L., Yoon, M., Motamedi, A., Kroll, A., Seo, C. P., Hsia, J. E., Kim, S. K., Mitchell, J. W. et al. (2015). Reversible centriole depletion with an inhibitor of Polo-like kinase 4. *Science* **348**, 1155-1160. doi:10.1126/science.aaa5111

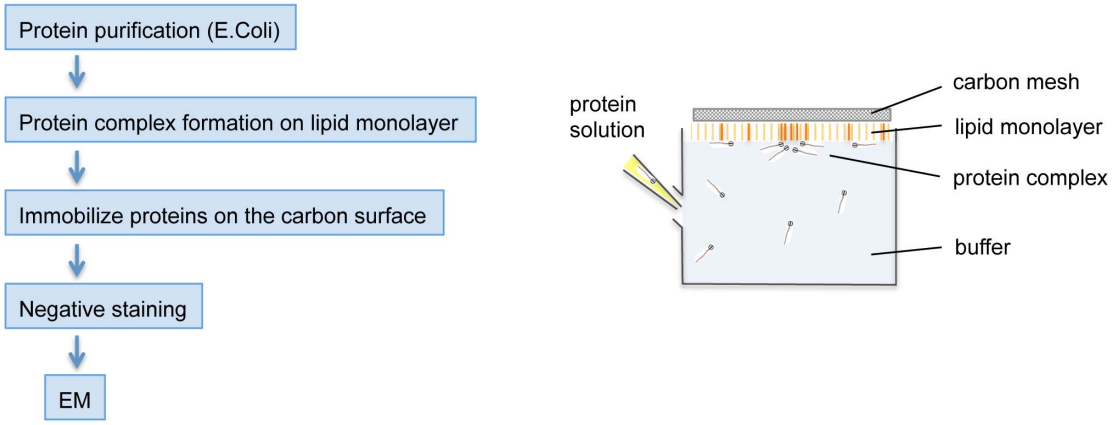

Figure S1. Experimental scheme of *in vitro* reconstitution of center part of cartwheel structure by HsSAS-6 fragment

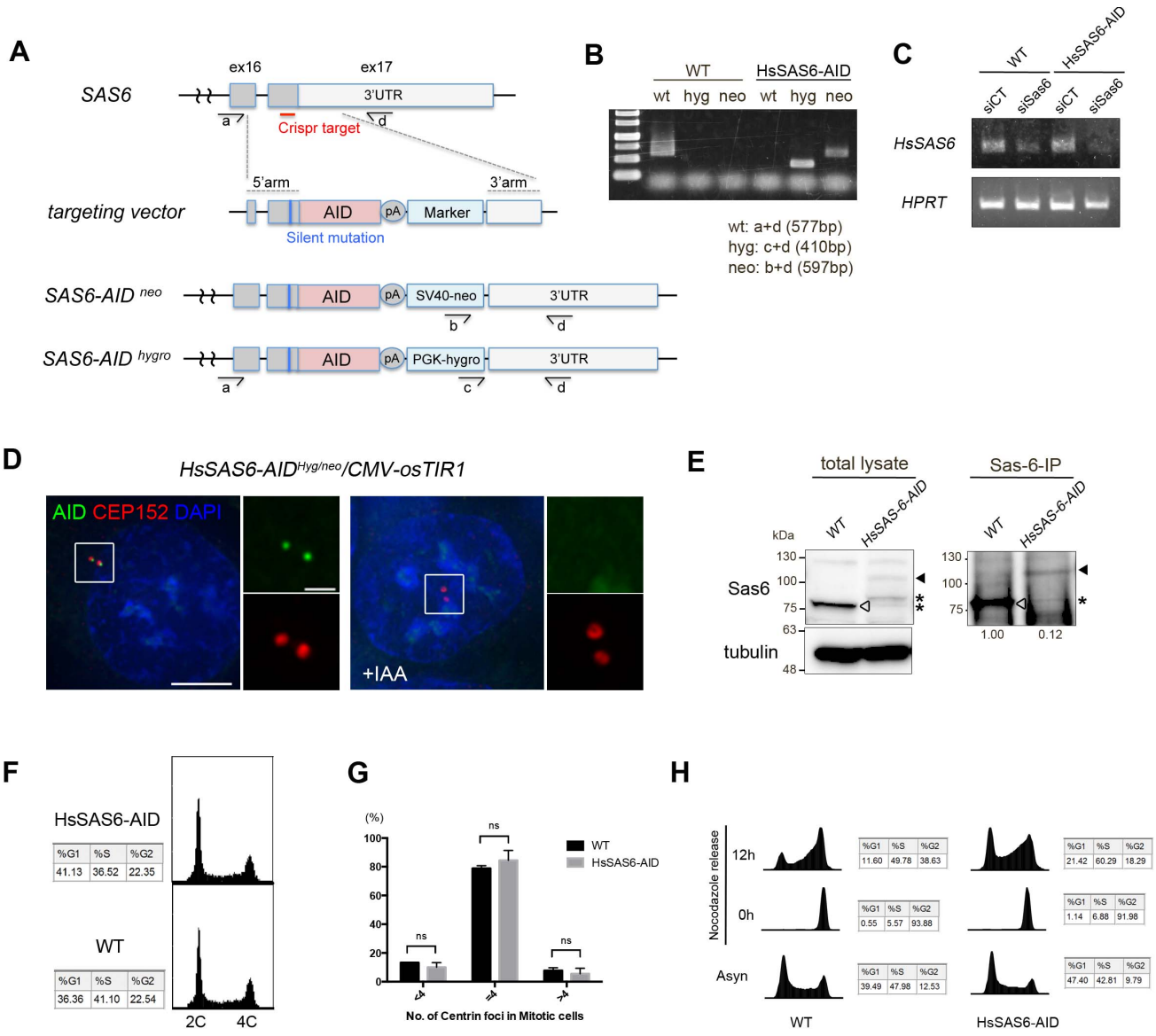

Figure S2. Generation of HsSAS-6-AID cell line

(A) Schematic representation of bi-allelic C-terminus AID-tagging on HsSAS-6 alleles by CRISPR/Cas9 system. Alphabets with arrows below the genes (A-D) indicate the positions of primers for genotyping used in B. (B) Bi-allelic AID knock-in was confirmed by genome PCR. Primer pairs used were indicated below. (C) Expression level of *HsSAS-6-AID* was semi-quantitatively tested by RT-PCR. *HsSAS-6* depletion by ORF-target *siHsSAS-6* reduced *HsSAS-6-AID* level, as is the case of *WT*. (D) The response to IAA in HsSAS-6-AID cell line was also confirmed by immunofluorescence with anti-AID antibody (related to Fig. 2A). (E) The amount of cytoplasmic HsSAS-6 protein was tested in WT and HsSAS-6-AID cells. Total lysates and IPs with anti-HsSAS-6 antibody were analyzed by western blotting using the indicated antibodies. White and black arrowheads point to endogenous HsSAS-6 and HsSAS-6-AID bands, respectively. The asterisk indicates a non-specific band. The blot and the signal intensities below shown are a representative from three independent experiments. (F)

HsSAS-6-AID cells show slightly more accumulation in G1 phase compared to WT cell by flow cytometry analysis. (G) Centriole duplication was normal in HsSAS-6-AID cell line. The number of centrin foci in mitotic cells was quantified. Values are mean percentages ± s.e.m. from three independent experiments (n ≥ 50 for each condition). The statistical significance between the data sets was determined by two-tailed unpaired *t*-test. ns, not significantly different ($p > 0.05$). (H) Cell cycle profile after nocodazole arrest release was tested in WT and HsSAS-6-AID cell lines. HsSAS-6-AID cells show a slight delay at 12hr after release compared to WT cells.

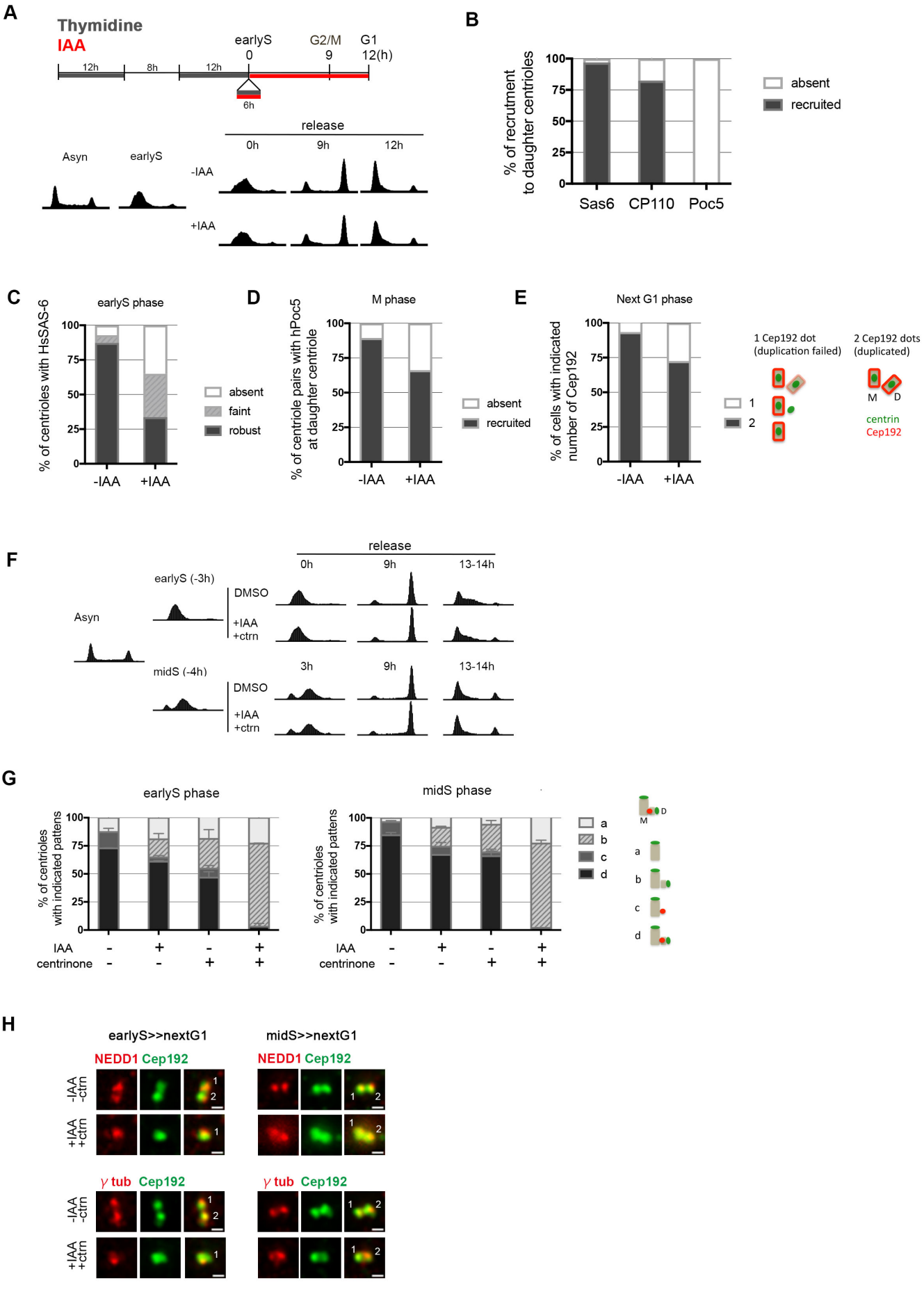

Figure S3. The effect of IAA on HsSAS-6-AID cell line

(A) Experimental scheme of HsSAS-6 removal in the S-phase arrested cells. Cells were synchronized at G1/S border (early S phase) by double thymidine block. For HsSAS-6-AID removal, cells were treated with 0.5 mM IAA for 6 h, and released into fresh medium with IAA until next G1. Cell cycle progression was monitored by flow cytometry (below). (B) Recruitment of HsSAS-6, CP110 and Poc5 at early S phase was tested. Values are mean percentages from two independent experiments (total n = 100, n = 34 and n = 50, respectively). (C) The number of centrosomes with HsSAS-6 after IAA treatment was quantified according to the indicated category. (D) The number of centriole pairs without or with hPoc5 at daughter centrioles at M phase was quantified. (E) The number of centrioles with the indicated number of Cep192 in the next G1 phase was quantified according to the patterns shown right. Values are mean percentages from two independent experiments (total n ≥ 100; C-E). (F) FACS profiles related to Fig. 4C-H are shown. After IAA and/or Centrinone treatment at early S phase or middle S phase, cells are released and proceed to next G1 phase within 13 to 14 h. (G) The number of centrioles with the indicated patterns after the drug treatment in Fig. 4D was quantified. Values are mean percentages from two independent experiments (total n ≥ 100). Left panel, in the early S phase; right panel, in the middle S phase. (H) Representative patterns of NEDD1 and γ-tubulin at next G1 phase after HsSAS-6 removal in the early S or middle S phase. Numbers in the panels indicate the number of mature centrioles.

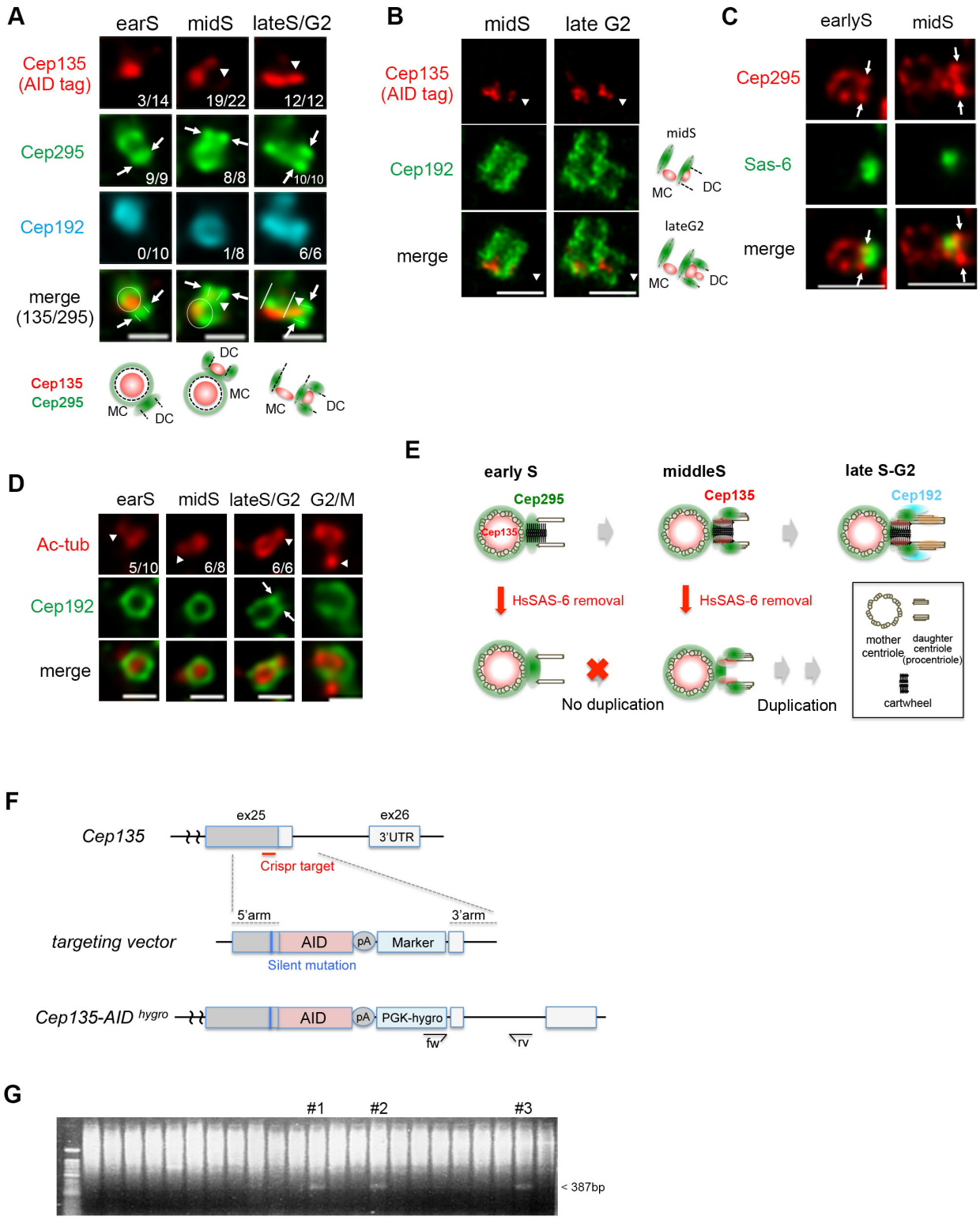

Figure S4. Ordered loading of centriolar proteins through earlyS phase to G2 phase in a growing procentriole.

(A) Loading of Cep295, Cep135 and Cep192 to procentrioles at the indicated stages was tested by immunofluorescence staining. Cep295 and Cep192 were detected by anti-Cep295 and anti-Cep192 antibodies, respectively. Cep135 was detected by anti-AID antibody against endogenously-tagged Cep135-AID (cell line information in F,G). Note that we also detected

similar patterns with anti-Cep135 antibody. The images were obtained by Leica TCS SP8 Hyvolution system. White arrowheads and white arrows indicate the signals of Cep135 and Cep295 at procentrioles, respectively. The numbers below represent the numbers of Cep135, Cep295 or Cep192 loading to procentrioles /total counts. Schematic illustrations are shown below. All scale bars in Figure S4, 500 nm. (B) Representative STED images of Cep135 loading to procentrioles in the middle S and late G2 phase. Schematic illustrations are shown on the right. (C) Representative STED images of Cep295 pattern at early and middle S phase. HsSAS-6 was used for a procentriole marker, and white arrows indicate procentriole sites. Notably Cep295 signals at procentriole sites seem to be increasing through early S to middle S phase. All scale bars in this figure, 500 nm. (D) Acetylation of tubulin in daughter centrioles was tested at the indicated stages. White arrowheads indicate procentriole assembly sites. Note that tubulin acetylation seems to occur earlier than other centriole maturation events, such as tubulin polyglutamylation and PCM recruitment. (E) Speculative illustration of the phenotypes by HsSAS-6 removal in the middle of procentriole formation. After Cep295 and Cep135 loading to the daughter centrioles, the cartwheel may be dispensable for further elongation and maturation. (F) Schematic representation of C-terminus AID-tagging on Cep135 allele by CRISPR/Cas9 system. The arrows below the gene (fw and rv) indicate the positions of primer pair for genotyping used in G. (G) Cep135-AID knock-in was screened by genomic PCR. Clone #1 was used in this study.

Table S1. Oligos used for the generation of HsSAS-6-AID and Cep135-AID cell lines.

Bold letters in guideRNAs show the sequence in the vector. Colored characters in 3' arm indicates the CRISPR/Cas9 target site. Note that PAM sequence is substituted, not to be targeted (Blue, guide RNA target site; green, part of PAM; red, substituted in PAM). BamHI site was inserted at the stop codon for the generation of targeting vector.

Gene	Oligo name	Sequence (5'-3')
HsSAS-6	gRNA fw	**CACCG**AATAGGCTGAAGACGCAGAG
	gRNA rv	**AAAC**CTCTGCGTCTTCAGCCTATT**C**
	3'arm	ttcctttacgcggactcagccagaacctatttagtaattcaggtaagcagggatt tctggatttttgtactttatagttgaattaaatttaatgtatgaagacttaatgaatac cagtaacctttttttgtcctcatttgcagaccatcagagagatggcactttagga gcattacatacatcttccaaacccacagcgctacctctgcgtcttcagcctat ttccctgggcagttaccaaacagt**ggatcc**ttctagtgtcatgttttacttttttatt ggtattttagaaactcaggtgcttaaaaaatatgtcaacacaaaccagatcctc aaatagcaagtttcaaattttacttgagctgttaaagactggatactttaagtact gcttttatggcagtttataatataggaacaaatttgtacttggggattggtaaagat tgtgagtaaatgacatttttttggtttgtgaacatggcgttttatagaataata
Cep135	gRNA fw	**CACCG**GACCATGTCGACGCATCTCT
	gRNA rv	**AAAC**AGAGATGCGTCGACATGGTC**C**
	3'arm	aaaattgtacaaagacataggatttaaatttaatagtaatactaagtaatttattac aaattagctaataactcttatatttgtttgccacttttgattttccctggtgcttgaat atatctctcttgtttgatctttactaacagagaacgagcaatacaagagatgcgt cgacatggtcttgctacaccacccctagttccactctgaggtctccttcacatt ctcctgaacatagaaatgtg**ggatcc**ttatcagaaaggtatgtatgtaacacc aaggacaggcaaaactaatctgtggttgtaaaaattcagaaagtagttttctgc atcaggaaaggggagattgcctggtaaggcgttcaggagaacttcctggagt aatggaaaagttctatatcttggtgatagtagttatgtgggtatatacaattgtaaa aattcataaaactgaccatttacagtgtatgctttttttttttttaagagatgggg